Nucleon structure with pion clouds in a flux-tube quark model

S. Kumano*
Department of Physics and Astronomy, University of Tennessee, Knoxville, Tennessee 37996-1200,
Physics Division, Oak Ridge National Laboratory, Oak Ridge, Tennessee 37831,
and Department of Physics, University of Illinois at Urbana-Champaign, Urbana, Illinois 61801
(Received 1 May 1989)

Nucleon structure with pion clouds is studied in the framework of a flux-tube quark model. The meson clouds are produced by breaking flux tubes in the nucleon; then a baryon is described by three valence quarks connected by color fields and other configurations including sea quarks. These sea quarks (or meson clouds) generate baryon decay widths and shift their masses; therefore, the hadron spectroscopy in constitutent-quark models should be investigated again by including these mass shifts. In this flux-tube model, the Yukawa potential is explained by a piece of the flux tube breaking off from a nucleon and attaching itself to the other.

I. INTRODUCTION

The MIT bag model[1] was successful in explaining basic static properties of the nucleon. In this model, large-distance effects of QCD are represented by the confinement of quarks in the bag, and short-distance effects are given by perturbation theory. From a nuclear physicist's point of view, one major difficulty with this model is explaining the well-known Yukawa potential. This problem is related to the nonconservation of the axial-vector current, and it was proposed that this issue could be solved if the pion couples to the nucleon so that the axial-vector current is conserved. This cloudy[2] (or chiral[3]) bag model was successful in explaining electromagnetic properties of the nucleon and reproducing pion-nucleon dynamics. However, one basic problem is that the pion is treated as an elementary field in contrast with the nucleon, although experimental charge radii of these particles are of the same order of magnitude. From the quark-model point of view, the pion must also be described in terms of quarks and gluons, so that the nucleon and its interactions could be described in terms of quark and gluon degrees of freedom.

A possible approach to this problem is to use the flux-tube quark model.[4,5] In this model, for example, a meson is treated as the interacting quark-antiquark pair and the color field connecting them. An extension of this model to meson decay has been investigated, and it gave a reasonable explanation for the strong decay of mesons,[6-8] even though there are still problems in the $q\bar{q}$ creation mechanism. References 7 and 9 use a $^3P_0$ $q\bar{q}$ creation model, and Ref. 6 uses a $^3S_1$ $q\bar{q}$ creation model. Decay widths calculated by both models are compared in Ref. 8. Discrepancies of these models arise typically in explaining the S-wave decay of the b_1 meson. Supporters of the $^3P_0$ model claim that this is a failure of the $^3S_1$ model because the calculated decay width is approximately 30 times larger than the experimental data.[7] However, if this large calculated decay width is reduced by the short-range, repulsive final-state interaction, due to quark-exchange effects,[10] the $^3S_1$ model should not be excluded.[8] Further investigations are needed to settle the $q\bar{q}$ creation mechanism in the flux tube. The $^3P_0$ model has been extended to the strong decay of baryons,[11,12] and it gives reasonable explanations for the pionic decay of baryons. It is interesting to investigate further the strong decay of baryons and to relate it to the nucleon structure research.

In this research I try to investigate $\pi N\Delta$ dynamics in terms of quark degrees of freedom as a first step to study baryon structure with sea quarks (meson clouds) in the flux-tube quark model. In Sec. II the πNN and the $\pi N\Delta$ couplings are derived from the flux-tube-breaking mechanism, and implications for the Δ decay width, its mass, and the Yukawa potential are discussed in Sec. III.

II. FLUX-TUBE BREAKING AND THE $\pi N\Delta$ SYSTEM

Both $^3S_1$ and $^3P_0$ models are applied to the nucleon structure problem. For details of the flux-tube-breaking mechanisms, I refer the reader to Refs. 6, 7, 8, and 9. In the following I briefly explain a basic approach. In the flux-tube model of Carlson, Kogut, and Pandharipande,[4] a baryon consists of three valence quarks and flux tubes connecting them. This flux-tube configuration depends on how the quarks are located, as shown in Fig. 1(a_i) and Fig. 1(b_i) (see Ref. 4 for details). By creation of a $q\bar{q}$ pair in the flux tube, a baryon (denoted as B) decays into an another baryon (B') and a meson (M), which is shown as the quark-antiquark and the flux tube connecting them in Fig. 1(a_f) and Fig. 1(b_f). This is the basic idea of creating "meson clouds" around a baryon. According to the flux-tube model, the Hamiltonian to create a $q\bar{q}$ pair is given by

$$\frac{\lambda^{\beta}_{ab}}{2}\frac{\lambda^{\beta}_{cj}}{2}\int dX_i \mathbf{F}\cdot\langle\chi'_i|\boldsymbol{\sigma}|\bar{\chi}'\rangle a^{\dagger}(X,\chi'_i)b^{\dagger}(X,\bar{\chi}')\ , \quad (2.1)$$

where $a^{\dagger}(X,\chi'_i)$ $[b^{\dagger}(X,\bar{\chi}')]$, $i=1,2,3$, is the quark [antiquark] creation operator at position X and spin state χ'_i $[\bar{\chi}']$, λ^{β} are color-SU(3) Gell-Mann matrices, and their

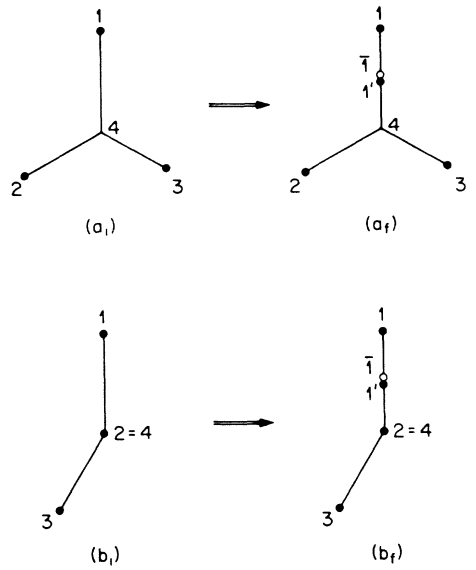

FIG. 1. Schematic figures of baryon decay. The flux tube is denoted by a line, and its configuration depends on how the quarks are located according to Ref. 4, as shown in (a_i) and (b_i). By the creation of a $q\bar{q}$ pair, the baryon decays into another baryon and a meson.

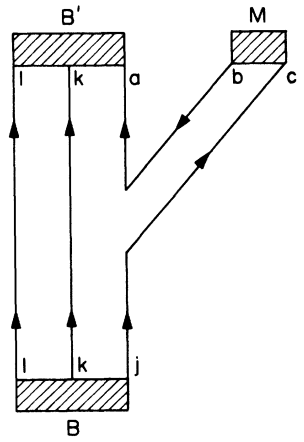

FIG. 2. Color indices of hadrons in a baryon decay.

color indices are shown in Fig. 2. In Eq. (2.1), the only upper (lower) component of the Dirac spinor is taken for the created quark (antiquark). $\mathbf{F}$ is an operator which depends on the model, and it is $\mathbf{F}=\Lambda_0\hat{\mathbf{r}}$ in the $^3S_1$ narrow flux-tube quark model,[6,8] where $\hat{\mathbf{r}}$ is the unit vector $(\mathbf{r}_i'-\mathbf{r}_4)/|\mathbf{r}_i'-\mathbf{r}_4|$ in Fig. 1(a_f) and Fig. 1(b_f) for $i=1$, and $\Lambda_0(\Lambda_0\equiv\Lambda/2,\Lambda$, as given in Ref. 8) is a strength to create the $q\bar{q}$ pair which is determined by fitting an experimental decay width, for example, $\Gamma(\rho\rightarrow\pi\pi)$. In this narrow flux-tube model, the integration in Eq. (2.1) is done along the straight line $\int dX_i=\int_{r_4}^{r_i'}dr$. In the $^3P_0$ model, the operator is $\mathbf{F}=\gamma(\mathbf{P}_q-\mathbf{P}_{\bar{q}})$ where $\mathbf{P}_q(\mathbf{P}_{\bar{q}})$ is the relative momentum of the created quark (antiquark), and γ is a pair creation constant. The integration is $\int dX_i=\int d^3r\,\gamma_i(\mathbf{r})$, where $\gamma_i(\mathbf{r})$ is a function to restrict the pair creation region in Ref. 7.

Using the above $q\bar{q}$ creation Hamiltonian, we have the matrix element of the baryon (B) decaying into a meson (M) and the baryon (B'):

$$\langle MB'|H_{\rm int}|B\rangle=C_0\sum_i[\langle MB'|\langle\chi_i'|\sigma|\bar{\chi}'\rangle a^\dagger(\chi_i')b^\dagger(\bar{\chi}')|B\rangle]_{\rm spin\,flavor}$$
$$\cdot\int d^3r_1d^3r_2d^3r_3\int dX_i\mathbf{F}\,\Psi^*_{MB'}(\mathbf{k},\mathbf{r}_i',\mathbf{r}_1,\mathbf{r}_2,\mathbf{r}_3)\Psi_B(\mathbf{r}_1,\mathbf{r}_2,\mathbf{r}_3)\ , \tag{2.2}$$

where $\Psi_B(\mathbf{r}_1,\mathbf{r}_2,\mathbf{r}_3)$ is the space part of the baryon (B) wave function, $\Psi_{MB'}(\mathbf{k},\mathbf{r}_i',\mathbf{r}_1,\mathbf{r}_2,\mathbf{r}_3)$ is the space part of the meson (M)-baryon (B') wave function, $\mathbf{k}$ is the relative momentum of the baryon (B') and the meson (M), and $\mathbf{r}_i'(i=1,2,3)$ is the position where the flux-tube breaking occurs. In this equation, C_0 is the color matrix element between color-singlet hadrons, and it is a constant given by

$$C_0\equiv\left[\left\langle M(cb)B'(lka)\left|\frac{\lambda_{ab}^\alpha}{2}\frac{\lambda_{cj}^\alpha}{2}\right|B(lkj)\right\rangle\right]_{\rm color}=\frac{4}{3\sqrt{3}}\ , \tag{2.3}$$

where color indices are shown in Fig. 2. Suppose the internal angular momenta of the baryons and the meson are $L=0$, we can take out the $\mathbf{k}$ dependence from the above spatial integral:

$$\int d^3r_1d^3r_2d^3r_3\int dX_i\mathbf{F}\,\Psi^*_{MB'}(\mathbf{k},\mathbf{r}_i',\mathbf{r}_1,\mathbf{r}_2,\mathbf{r}_3)\Psi_B(\mathbf{r}_1,\mathbf{r}_2,\mathbf{r}_3)=A_{MB'B}(k)\mathbf{k}\ , \tag{2.4}$$

where $A_{MB'B}(k)$ is defined by

$$A_{MB'B}(k)=\int d^3r_1d^3r_2d^3r_3\int dX_1\frac{\hat{\mathbf{k}}\cdot\mathbf{F}}{k}\Psi^*_{MB'}(\mathbf{k},\mathbf{r}_1',\mathbf{r}_1,\mathbf{r}_2,\mathbf{r}_3)\Psi_B(\mathbf{r}_1,\mathbf{r}_2,\mathbf{r}_3)\ . \tag{2.5}$$

In this paper I study exclusively the $\pi N\Delta$ system which is important in nucleon structure research. Hereafter, B and B' denote the nucleon or the Δ. Using the pion spin-flavor wave function[13], we obtain

$$[\langle \pi B'|\langle \chi_i'|\sigma|\bar{\chi}'\rangle a^\dagger(\chi_i')b^\dagger(\bar{\chi}')|B\rangle]_{\text{spin flavor}}=\frac{\tilde{\phi}_\pi^*}{2}\cdot\left[\left\langle B'\left|\sum_i \bar{\tau}(i)\sigma(i)\right|B\right\rangle\right]_{\text{spin flavor}}, \tag{2.6}$$

where $\tilde{\phi}_\pi$ is the pion isospin vector, and $\sigma(i)$ and $\bar{\tau}(i)$ are Pauli spin and isospin operators on the i quark. In deriving this equation we should be careful about the phase convention of the antiquark. Using the nucleon and the Δ spin-flavor wave functions,[13] we obtain

$$\left\langle B'\left|\sum_i \bar{\tau}(i)\sigma(i)\right|B\right\rangle = N_B N_{B'}\frac{6\sqrt{(2J+1)(2T+1)(2J'+1)(2T'+1)}}{\langle J'\|\hat{S}\|J\rangle\langle T'\|\hat{T}\|T\rangle}\langle J'M_J'|\mathbf{S}|JM_J\rangle\langle T'M_T'|\tilde{T}|TM_T\rangle$$
$$\times\sum_{j,j'=0,1}\left[(-1)^{1+J'+T'}\delta_{jj'}\begin{Bmatrix} J & \frac{1}{2} & j \\ \frac{1}{2} & J' & 1\end{Bmatrix}\begin{Bmatrix} T & \frac{1}{2} & j \\ \frac{1}{2} & T' & 1\end{Bmatrix}\right.$$
$$\left.+(-1)^{1+J+T}2(2j+1)(2j'+1)\begin{Bmatrix} j & \frac{1}{2} & \frac{1}{2} \\ \frac{1}{2} & 1 & j'\end{Bmatrix}^2\begin{Bmatrix} j' & j & 1 \\ J & J' & \frac{1}{2}\end{Bmatrix}\begin{Bmatrix} j' & j & 1 \\ T & T' & \frac{1}{2}\end{Bmatrix}\right], \tag{2.7}$$

where N_B is the normalization constant given by $N_N=1/\sqrt{2}$ and $N_\Delta=1$, and $\mathbf{S}$ is defined by

$$\langle J'M_{J'}|\mathbf{S}|JM_J\rangle = \sum_M \frac{\langle J'||\hat{S}||J\rangle}{\sqrt{2J'+1}}\langle JM_J:1M|J'M_{J'}\rangle\epsilon_m^*, \tag{2.8}$$

where ϵ_m^* is the spherical unit vector.[14] The matrix element of isospin $\tilde{T}$ is defined in the same way. Defining the reduced matrix elements in the nucleon and Δ system by

$$\langle \tfrac{1}{2}||\hat{S}||\tfrac{1}{2}\rangle=\sqrt{6},$$
$$\langle \tfrac{3}{2}||\hat{S}||\tfrac{1}{2}\rangle=2, \tag{2.9}$$
$$\langle \tfrac{3}{2}||\hat{S}||\tfrac{3}{2}\rangle=\sqrt{15},$$

in the same way for the reduced matrix elements of $\tilde{T}$, we obtain

$$\left\langle B'\left|\sum_i \bar{\tau}(i)\sigma(i)\right|B\right\rangle=\tfrac{5}{3}D_{B'B}\langle B'|\tilde{T}\mathbf{S}|B\rangle, \tag{2.10}$$

where constant $D_{B'B}$ is given by

$$D_{NN}=1,\quad D_{\Delta N}=(\tfrac{72}{25})^{1/2},\quad D_{\Delta\Delta}=\tfrac{4}{5}. \tag{2.11}$$

This is the well-known SU(6) symmetry for the coupling constants in the $\pi N\Delta$ system.

Substituting Eqs. (2.4), (2.6), and (2.10) into Eq. (2.2), we get the flux-tube-breaking interaction responsible for the $B\to B'\pi$ transition:

$$\langle \pi B'|H_{\text{int}}|B\rangle = C_0 A_{\pi B'B}(k)\tfrac{5}{6}D_{B'B}\langle B'|\tilde{\phi}_\pi^*\cdot\tilde{T}\mathbf{k}\cdot\mathbf{S}|B\rangle. \tag{2.12}$$

We define the semirelativistic (SR) matrix element by taking into account the $\sqrt{m/E}$ factor:[8]

$$[\langle \pi B'|H_{\text{int}}|B\rangle]_{\text{SR}}=\left[\frac{m_{B'}m_\pi}{E_{B'}\omega_\pi}\right]^{1/2}\langle \pi B'|H_{\text{int}}|B\rangle \tag{2.13}$$

and define the $\pi B'B$ vertex by $V_{\pi B'B}(\mathbf{k})=[\langle \pi B'|H_{\text{int}}|B\rangle]_{\text{SR}}/(2\pi)^{3/2}$. This is conventionally written as

$$V_{\pi B'B}(\mathbf{k})=\frac{\sqrt{4\pi}}{(2\pi)^{3/2}\sqrt{2\omega_\pi}}\frac{f_{\pi B'B}}{m_\pi}h_{\pi B'B}(k)\mathbf{k}\cdot\mathbf{S}\tilde{\phi}_\pi^*\cdot\tilde{T}. \tag{2.14}$$

Comparing these equations, we obtain the $\pi B'B$ coupling constants

$$f_{\pi B'B}=\frac{m_\pi^{3/2}}{\sqrt{2\pi}}\frac{5}{6}C_0 D_{B'B}|A_{\pi B'B}(k=0)| \tag{2.15}$$

and the $\pi B'B$ form factors

$$h_{\pi B'B}(k)=\left[\frac{m_{B'}}{E_{B'}}\right]^{1/2}\frac{|A_{\pi B'B}(k)|}{|A_{\pi B'B}(k=0)|}. \tag{2.16}$$

In the Kokoski-Isgur (KI) model, $m_\pi^{3/2}$ in Eq. (2.15) should be replaced by $m_\pi^{3/2}\sqrt{\tilde{m}_\pi\tilde{m}_{B'}/(m_\pi m_{B'})}$, where $\tilde{m}_\pi$ and $\tilde{m}_{B'}$ are the pion and baryon B' masses without the spin-dependent quark potential. For example, they are $\tilde{m}_\pi=720$ MeV (Ref. 7) and $\tilde{m}_N=1141$ MeV (Ref. 4). In this way, coupling constants and form factors in the $\pi N\Delta$ system are derived in the flux-tube quark model.

III. RESULTS

A. Numerical calculation method

Variational nucleon and Δ wave functions in Ref. 4 are used for the numerical evaluation of the πNN and $\pi N\Delta$ couplings derived in the last section. We should be careful to normalize the wave functions in order to calculate the $\pi N\Delta$ vertex. The pion radius in the flux-tube quark model is small, so that its wave function is approximated by the Coulomb wave function $\phi_\pi(r)=C_\pi e^{-\mu_\pi r}$, where C_π and μ_π are given by the pion rms radius R_π, as $\mu_\pi=\sqrt{3}/(2R_\pi)$ and $C_\pi=\mu_\pi^{3/2}/\sqrt{\pi}$. Because the nucleon and Δ wave functions are given by several variational parameters, we need to do ten- or twelve-dimensional numerical integration by the Monte Carlo method. The Metropolis method[15] is used to sample the probability distribution $D(\mathbf{r}_1',\mathbf{r}_1,\mathbf{r}_2,\mathbf{r}_3)$ and generate a set $(\mathbf{r}_1',\mathbf{r}_1,\mathbf{r}_2,\mathbf{r}_3)$. In the flux-tube (FT) model, the distribution function is

chosen as $D(\mathbf{r}_1,\mathbf{r}_2,\mathbf{r}_3)=[\Psi_B(\mathbf{r}_1,\mathbf{r}_2,\mathbf{r}_3)]^2$. In the flux-volume (FV) model, it is $D(\mathbf{r}'_1,\mathbf{r}_1,\mathbf{r}_2,\mathbf{r}_3)=(\mu_0/\pi)^{3/2}\times e^{-\mu_0(\mathbf{r}'_1-\mathbf{r}_{\text{c.m.}})^2}[\Psi_B(\mathbf{r}_1,\mathbf{r}_2,\mathbf{r}_3)]^2$. The constant μ_0 is chosen to provide a good accuracy for the numerical integration, and $\mu_0=5.0/\text{fm}^2$ is used. Taking 50 000 random points for the integration, we obtain a numerical accuracy of better than 5%.

The final-state wave function in Eq. (2.5) is

$$\Psi_{\pi N}(\mathbf{k},\mathbf{r}'_1,\mathbf{r}_1,\mathbf{r}_2,\mathbf{r}_3)=\phi_\pi(r_\pi)\Psi_N(\mathbf{r}'_1,\mathbf{r}_2,\mathbf{r}_3)\sum_l (i)^l(2l+1)u_l(kr_{\pi N})P_l(\hat{\mathbf{k}}\cdot\hat{\mathbf{r}}_{\pi N}) , \tag{3.1}$$

where $\mathbf{r}_{\pi N}$ is the πN relative coordinate, $P_l(\hat{\mathbf{k}}\cdot\hat{\mathbf{r}}_{\pi N})$ is the Legendre polynomial of order l, and $u_l(kr_{\pi N})$ is the πN relative wave function. In Ref. 8 we assumed a hard-core final-state interaction between mesons, which could be justified as a quark-exchange effect. The same kind of feature is expected for the short-range part of the pion-nucleon final-state interaction; in fact, the hard-core size (0.42 ± 0.11 fm) is used to explain the low-energy S-wave experimental data.[16] In this paper the hard-core final-state interaction between the pion and the nucleon with radius $C_{\pi N}$ is assumed to take into account this feature. In this description, the relative wave function is

$$u_l(kr_{\pi N}) = \begin{cases} \cos\delta_l j_l(kr_{\pi N})-\sin\delta_l n_l(kr_{\pi N}) & \text{for } r_{\pi N}>C_{\pi N}, \\ 0 & \text{for } r_{\pi N}<C_{\pi N}, \end{cases} \tag{3.2}$$

where $j_l(kr_{\pi N})$ and $n_l(kr_{\pi N})$ are the spherical Bessel and spherical Neumann functions, and the phase shift δ_l is given by the hard-core radius $C_{\pi N}$ as

$$\tan\delta_l=\frac{j_l(kC_{\pi N})}{n_l(kC_{\pi N})} . \tag{3.3}$$

The operator $\mathbf{F}$ in Eq. (2.5) is given by taking $\hat{\mathbf{k}}=\hat{\mathbf{z}}$:

$$\frac{\hat{\mathbf{k}}\cdot\mathbf{F}}{k}=\Lambda_0\frac{\hat{\mathbf{z}}\cdot\hat{\mathbf{r}}_{14}}{k} \quad \text{in the } {}^3S_1 \text{ model} , \tag{3.4}$$

$$\frac{\hat{\mathbf{k}}\cdot\mathbf{F}}{k}=-\gamma_0(\text{or } \bar{\gamma}_0)\left(1+i\frac{2\mu_\pi}{k}\frac{z_1-z'_1}{|\mathbf{r}_1-\mathbf{r}'_1|}\right) \quad \text{in the } {}^3P_0 \text{ model} . \tag{3.5}$$

At first, the core radius $C_{\pi N}$ is determined to obtain the πNN coupling constant $f_{\pi NN}$. As discussed in Sec. II both the ${}^3S_1$ and ${}^3P_0$ models are examined. We also examine the location where the pair creation occurs. In the flux-tube (FT) model, the $q\bar{q}$ pair creation occurs within the straight line connecting $\mathbf{r}_1$ and $\mathbf{r}_4$, as shown in Fig. 1. On the other hand, the pair is created anywhere in the neighborhood of parent quarks in the flux-volume (FV) model. Furthermore, in order to examine how the results depend on the pion radius, numerical results are shown for $R_\pi=0.16$ and 0.29 fm. Note that the effects of color-magnetic interaction on hadron wave functions are not very significant except for the pion case. The pion rms radius shrinks to 0.16 fm from 0.29 fm due to color-magnetic interaction.[4]

In Sec. III B, results for the coupling constant $f_{\pi N\Delta}$ and the form factor $h_{\pi N\Delta}(k)$ are presented and flux-tube-breaking effects on the Δ mass are discussed. In sec. III C, results for the πNN coupling are presented, and a possible explanation for the Yukawa potential is discussed. In Sec. III D, the results are summarized.

B. Δ decay width and mass shift

By using the $\pi N\Delta$ couplings derived in the last section, we can study electromagnetic properties of the nucleon and the Δ not only in the valence-quark part but also in the sea quarks (pion clouds). For example, the sea quarks (pion clouds) could have a dominant effect on the $N\to\Delta$ transition $E2/M1$ ratio.[17] These sea quarks also carry some of the nucleon spin by orbital angular momenta.[18] These problems are currently controversial issues. Furthermore, strong interactions of the nucleon and the Δ can also be investigated. The pion clouds play a crucial role in the strong-interaction dynamics. As an example, the Δ mass shift and its decay width are discussed in this section. We know that a possible way to explain the πN elastic scattering data in the P_{33} channel is to couple the bare Δ to the πN continuum.[19] Then, the physical Δ propagator shown in Fig. 3 is given in terms of the self-energy as $G_\Delta(E)=1/[E-m_\Delta-\Sigma_\Delta(E)]$, and the self-energy is [20]

$$\Sigma_\Delta(E)=\sum_B\int d^3p\frac{V^\dagger_{\pi B\Delta}(\mathbf{p})V_{\pi B\Delta}(\mathbf{p})}{E^+-\omega_{\mathbf{p}}-E^B_{-\mathbf{p}}} , \tag{3.6}$$

where the intermediate baryon (B) can be N, Δ, N^*, etc. However, the πN is the only open channel in the Δ resonance region which provides the imaginary part of the Δ self-energy. Expressing the above integral in terms of the Cauchy principal integration and the delta function, we have the real part which provides the Δ mass shift on resonance $E_R=1232$ MeV:

$$\delta m_\Delta=\text{Re}\Sigma_\Delta(E_R)=\sum_B P\int d^3p\frac{V^\dagger_{\pi B\Delta}(\mathbf{p})V_{\pi B\Delta}(\mathbf{p})}{E_R-\omega_{\mathbf{p}}-E^B_{-\mathbf{p}}} , \tag{3.7}$$

and we have the imaginary part for the Δ width:

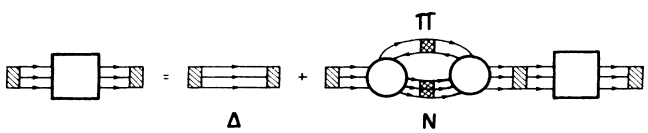

FIG. 3. Physical Δ propagator in the flux-tube quark model.

$$\Gamma_\Delta = -2\,\mathrm{Im}\Sigma_\Delta(E_R) = \frac{2\pi q^2}{\partial E/\partial q}\int d\Omega_q V^\dagger_{\pi N\Delta}(\mathbf{q})V_{\pi N\Delta}(\mathbf{q}) , \quad (3.8)$$

where $q \equiv |\mathbf{q}|$ is given by $E_R = \omega_q + E^N_{-q}$. This decay width is equivalent to the one calculated by the first-order perturbation theory using the flux-tube-breaking Hamiltonian in Eq. (2.2) or Eq. (2.12):

$$\Gamma_\Delta = \frac{1}{(2T_\Delta+1)(2J_\Delta+1)}\sum_{M_{T_N}}\sum_{M_{J_N}}\sum_{M_{T_\Delta}}\sum_{M_{J_\Delta}}\int\frac{d^3q}{(2\pi)^3}\delta(E_R-\omega_q-E^N_{-q})2\pi|[\langle\pi N|H_{\mathrm{int}}|\Delta\rangle]_{\mathrm{SR}}|^2 . \quad (3.9)$$

This lowest-order estimate would be sufficient at the present level of sophistication in the flux-tube model. The flux-tube quark models[4,5,21,22] studied for hadron spectroscopy agree that the nucleon and Δ rms radii are of the order of 0.4 fm, which roughly corresponds to the MIT bag-type confinement radius of 0.8 fm. The cloudy-bag model of this radius (0.8 fm) explains the Δ decay width by including second-order pion effects.[23] If the confinement radius were large as 1.4 fm (rms radius 0.7 fm), the first-order pion effect would be enough to explain the Δ width as it is done in the isobar model.[19] Therefore as the confinement radius, or the rms radius, becomes smaller, many pionic effects become more important and the perturbation approach becomes invalid. However, the fact that the rms radius, 0.4 fm, calculated in the flux-tube quark models is not very small, implies that the perturbation approach is not nonsense.

At first, the core radius of the final πN interaction is adjusted to obtain the πNN coupling constant $f^2_{\pi NN}=0.08$, and the results are shown in Table I. In the $^3S_1$-FT-KI model with $R_\pi=0.29$ fm, the $^3P_0$-FT-SR and KI models with $R_\pi=0.29$ fm, and the $^3P_0$-FV-KI model with $R_\pi=0.29$ fm, it is impossible to obtain the coupling constant ($f^2_{\pi NN}=0.08$) by the repulsive final-state interaction. Therefore, results are shown by taking $C_{\pi N}=0$ fm (no final-state interaction). The required core size is larger in the $^3S_1$ model ($C_{\pi N}=0.288$ fm for $R_\pi=0.29$ fm) than in the $^3P_0$ model ($C_{\pi N}=0$ fm). Considering the fact that we use the core radius 0.42 ± 0.11 fm (Ref. 16) for the πN interaction, we find that the $^3S_1$-FT-SR model with $R_\pi=0.16$, 0.29 fm, the $^3P_0$-FT-SR model with $R_\pi=0.16$ fm, and the $^3P_0$-FV-SR model with $R_\pi=0.16$ fm have core radii of the order of this value. In these models, calculated Δ widths agree well with the experimental value 116 MeV. In the $^3P_0$-FT and FV-SR models with $R_\pi=0.29$ fm, the width is underestimated by 40%. This is similar to the cloudy-bag-model[2,23] case, in which the Δ width is underestimated in the first-order calculation if the πNN coupling constant is chosen to be $f^2_{\pi NN}=0.08$. We also find that it is impossible to explain the Δ width by the $^3P_0$-FT and FV-KI models if we choose $R_\pi=0.29$ fm.

We find in Table I that $C_{\pi N}$ is very small (0.014 fm) in the $^3P_0$-FV-SR model with $R_\pi=0.29$ fm (model 8). This means that the πNN coupling constant could be explained without the final-state interaction if we adjust the pair creation constant (γ_0) to fit the $\rho\to\pi\pi$ decay width. Therefore, the results agree with the fact that the naive $^3P_0$ $q\bar{q}$ pair creation model has been successful without any final-state interaction as investigated by Le Yaouanc *et al.*,[9] Stancu and Stassart,[11] and Miller.[12] This research

TABLE I. Parameters in the flux-tube-breaking models. Coupling constants were determined to fit the $\rho\to\pi\pi$ decay width in Ref. 8. The hard-core size of the πN interaction, $C_{\pi N}$, is determined to obtain $f^2_{\pi NN}=0.08$. From the coupling constants ($f_{\pi NN}$,$f_{\pi N\Delta}$) and the form factors ($h_{\pi NN}(k)$,$h_{\pi N\Delta}$)) in Table II, the Δ width and the Δ and nucleon mass shifts (δm_Δ,δm_N) are calculated. $\delta m_{\Delta-N}$ is the mass-shift difference, $\delta m_\Delta-\delta m_N$. α_2 is determined by $h(k=\sqrt{\sqrt{2}-1}\,\alpha_2)=\frac{1}{2}$ in order to compare with the conventional form factor used in nuclear physics. $^3S_1$ ($^3P_0$) denotes the $^3S_1$ ($^3P_0$) $q\bar{q}$ pair creation model, FT: flux-tube, FV: flux-volume, SR: semirelativistic, and KI:Kokoski-Isgur. See text for explanations of these models.

	Model	Coupling	R_π (fm)	$C_{\pi N}$ (fm)	Γ_Δ (GeV)	$\delta m_\Delta^{(\pi N)}$ (GeV)	$\delta m_{\Delta-N}^{(\pi N)}$ (GeV)	$f_{\pi N\Delta}$	$\alpha_2^{\pi N\Delta}$ (1/fm)	$f_{\pi NN}$	$\alpha_2^{\pi NN}$ (1/fm)
		Λ_0(fm)									
(1)	$^3S_1$-FT-SR	79.0	0.16	0.441	0.13	−0.42	−0.02	0.739	4.9	fitted	4.9
(2)	$^3S_1$-FT-SR	31.1	0.29	0.288	0.12	−0.44	+0.06	0.679	5.9	fitted	6.1
(3)	$^3S_1$-FT-KI	5.85	0.29	0.000	0.072	−0.32	+0.22	0.504	7.2	0.241	7.7
		$\overline{\gamma}_0$(fm)^2									
(4)	$^3P_0$-FT-SR	2.24	0.16	0.292	0.11	−0.53	+0.21	0.646	6.3	fitted	6.4
(5)	$^3P_0$-FT-SR	1.48	0.29	0.000	0.064	−0.23	+0.22	0.481	6.6	0.250	7.1
(6)	$^3P_0$-FT-KI	0.279	0.29	0.000	0.014	−0.05	+0.05	0.227	6.6	0.118	7.1
		γ_0									
(7)	$^3P_0$-FV-SR	7.55	0.16	0.205	0.11	−0.86	+0.86	0.609	8.5	fitted	9.1
(8)	$^3P_0$-FV-SR	1.97	0.29	0.014	0.073	−0.30	+0.48	0.510	7.0	fitted	7.7
(9)	$^3P_0$-FV-KI	0.370	0.29	0.000	0.018	−0.07	+0.11	0.250	6.9	0.140	7.6

extends their research by investigating other factors, such as the different $q\bar{q}$ pair creation models ($^3P_0$ and $^3S_1$), the position of the pair creation (FT and FV), the pion rms radius (R_π), and the final-state interaction. In model 5 we find that the $\pi N\Delta$ coupling constant is 7% larger than the SU(6) value ($f_{\pi N\Delta}=6\sqrt{2}f_{\pi NN}/5$), and this is in agreement with their research (e.g., Ref. 12). However, we should note that 30–50% enhancement factors are obtained in the other models, 1, 2, 4, and 7, as listed in Table I, and these enhancements of $f_{\pi N\Delta}$ make the calculated Δ decay widths agree with the experimental value.

In the zeroth-order flux-tube model spectroscopy,[4,21,22] the magnitude of the color coupling constant α_c is chosen so that the spin-spin interaction provides the $N-\Delta$ mass difference. In this research, I investigate sea-quark (or meson-cloud) effects which have been neglected in the valence-quark models. If the meson clouds are taken into account, the Δ "bare" mass which should have been fitted by the zeroth-order model is not 1232 MeV but it is larger,[19,23,24] 1232 MeV$-\delta m_\Delta$, where the Δ mass shift δm_Δ is negative. We should note that the nucleon also acquires a mass shift δm_N. These mass shifts, which come from the πN channel [e.g., $B=N$ in Eq. (3.7)], are calculated by assuming the πN final-state interaction which is adjusted to fit the πNN coupling constant, as listed in Table I. The form factors are evaluated at $k=0,1,2,3,4,5,6,8,10,12,14,16,18,20$/fm by the Monte Carlo method, and the normalized ones are fitted by a simple function $1/(1+k^2/\alpha_n)^n$. The form factor for the $^3S_1$-FT-SR model with $R_\pi=0.29$ fm is shown as an example in Fig. 4. α_n and n are obtained to fit the shape of the form factor, and they are shown in Table II. In order to compare with the conventional cutoff parameters, we calculate α_2 so as to satisfy $h(k=\sqrt{\sqrt{2}-1}\alpha_2)=\frac{1}{2}$. Discussions on the cutoff parameter α_2 are made in Sec. III C. Using listed coupling constants ($f_{\pi N\Delta}$ and $f_{\pi NN}$ in Table I) and form factors [$h_{\pi N\Delta}(k)$ and $h_{\pi NN}(k)$ in Table II], we obtain the mass shifts shown in Table I. Depending on the model, the Δ and nucleon mass shifts are obviously between -200 and -800 MeV, except for the $^3P_0$-FV-SR model with $R_\pi=0.16$ fm. These results are expected from the nucleon size we have in the flux-tube model. This nucleon (and pion) size determines an approximate value for the cutoff parameter α_n. Therefore, we can reasonably expect that the absolute value of the mass shift in the flux-tube model is larger than that in the isobar model[19] (90–213 MeV), and it is roughly equal to a cloudy-bag-model value (319 MeV) calculated by Johnstone and Lee.[23] Obtained mass shifts agree with Nogami and Ohtsuka's results[25] by noting that a relation between their cutoff parameter (Λ) and the one used in this research (α_2), $\Lambda\approx 0.55\alpha_2\approx 5./m_\pi$ for $\alpha_2=6.5$/fm.

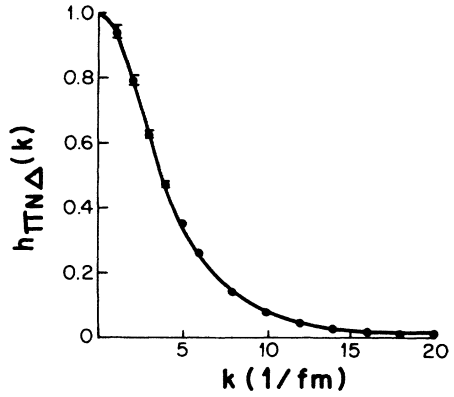

FIG. 4. The $\pi N\Delta$ form factor for the $^3S_1$-FT-SR model with $R_\pi=0.29$ fm and $C_{\pi N}=0.288$ fm is shown as an example. Monte Carlo results of the $\pi N\Delta$ form factor are shown by the filled circles with error bars. The solid line is the fitting by $1/(1+k^2/\alpha_n^2)^n$ with $n=1.69$ and $\alpha_n=5.37$/fm.

TABLE II. Calculated form factors are fitted by the function $h(k)=1/(1+k^2/\alpha_n^2)^n$. These form factors are used to evaluate the Δ decay width and the Δ and nucleon mass shifts. See Table I and text for explanations of the models.

Model	$n^{\pi N\Delta}$	$\alpha_n^{\pi N\Delta}$ (1/fm)	$n^{\pi NN}$	$\alpha_n^{\pi NN}$ (1/fm)
(1)	1.12	3.40	1.10	3.36
(2)	1.69	5.37	1.57	5.23
(3)	9.21	16.62	5.40	13.43
(4)	1.31	4.86	1.22	4.74
(5)	6.50	12.60	6.00	13.01
(6)	6.50	12.60	6.00	13.01
(7)	1.71	7.69	1.42	7.34
(8)	8.33	15.34	3.60	10.81
(9)	10.32	16.79	4.18	11.50

Calculated Δ mass shifts and $N-\Delta$ mass shift differences due to the πN intermediate state are listed in Table I. It is impossible to draw any conclusions about validity of the zeroth-order hadron spectroscopy unless we calculate the mass shifts as coming from all possible intermediate states. However, the mass shift differences ($\delta m_{\Delta-N}^{\pi N}$) listed in Table I give some indications. At first, we notice that they are very dependent on details of the model, such as the pion size, the location of a $q\bar{q}$ pair creation, and the state in which the pair is created. They are not very large (0–200 MeV) in the flux-tube (FT) creation model, however, they are large (500–900 MeV) in the flux-volume (FV) model. Because the calculated mass shift differences are not, in general, small compared with the $N-\Delta$ mass difference (292 MeV), the whole zeroth-order hadron spectroscopy should be repeated by taking into account the mass shifts due to the sea-quark (or the meson-cloud) effects.

C. Yukawa potential

In the flux-tube model, the Yukawa potential could be understood easily by the flux-tube-breaking mechanism. At first, the πNN coupling is evaluated and results are shown in Table I. The conventional πNN form factor used in nuclear physics is $1/(1+k^2/\alpha_2^2)^2$, and the cutoff parameter is usually taken to be $\alpha_2=4$–6/fm (Ref. 26).

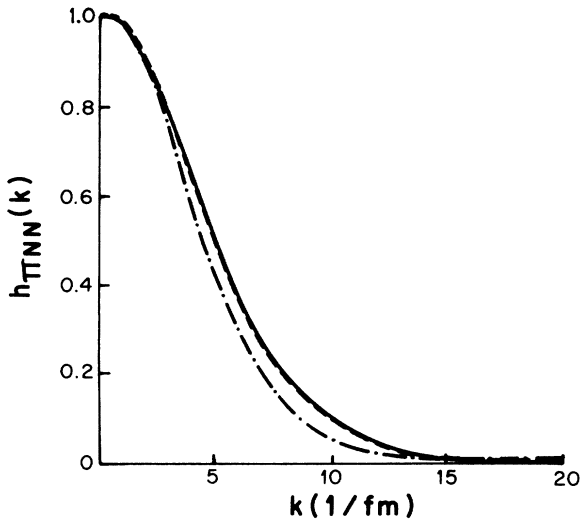

FIG. 5. Model dependences of the πNN form factor with $R_\pi=0.29$ fm and $C_{\pi N}=0$ fm are shown. The solid line shows the interpolated form factor by the $^3S_1$-FT model ($\alpha_2=7.7$/fm), the dashed line by the $^3P_0$-FV model ($\alpha_2=7.6$/fm), and the dashed-dotted line by the $^3P_0$-FT model ($\alpha_2=7.1$/fm).

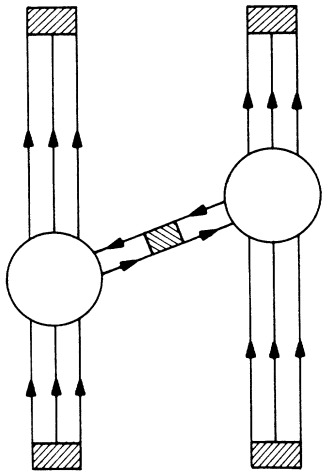

FIG. 7. Schematic figures of the Yukawa potential. A piece of flux tube is broken off from a nucleon, the flux-tube propagates as a pion, and it is attached to the other nucleon.

We calculate the parameter α_2 so as to satisfy $h_{\pi NN}(k=\sqrt{\sqrt{2}-1}\alpha_2)=\frac{1}{2}$ in the flux-tube model. The α_2 so obtained for all the models is listed in Table I. These results for α_2 indicate that the cutoff parameters by almost all models considered here are close to the conventional value (4–6/fm). However, the cutoff values in the $^3P_0$ model ($\alpha_2\approx 7$/fm) are larger than the conventional vlaues. In Table I, the obtained cutoff parameter is smaller in the $^3S_1$ model ($\alpha_2=6.1$/fm for $R_\pi=0.29$ fm) than in the $^3P_0$ ($\alpha_2=7.1$/fm), and also smaller in the flux-tube (FT) model ($\alpha_2=7.1$/fm) than in the flux-volume (FV) ($\alpha_2=7.7$/fm). We should note that the above argument is for the different final-state interaction adjusted to fit the πNN coupling constant in each model. In the case of no final-state interaction ($C_{\pi N}=0$ fm), model dependences of the πNN form factor are shown in Fig. 5, where the pion rms radius is fixed at 0.29 fm. In Fig. 5 we find that the form factor is softer in the $^3P_0$-FT model than the one in the $^3S_1$-FT, and the difference is $\delta\alpha_2=0.6$/fm. The form factor in the $^3P_0$-FV model is harder ($\delta\alpha_2=0.5$/fm) than the one in the $^3P_0$-FT model. From these results, we find that the form factor is not significantly dependent on the model ($^3S_1$, $^3P_0$, FT, FV) we use. Dependences on the final-state interaction and the pion radius are shown in Fig. 6, where the $^3S_1$-FT model is taken as an example. If the pion radius is smaller ($R_\pi=0.29\rightarrow 0.16$ fm), the form factor becomes slightly harder ($\delta\alpha_2=0.4$/fm). The effects of a repulsive final-state interaction are significant compared with others (pion radius, $q\bar{q}$ creation models); in fact, the repulsive interaction with a core radius 0.288 fm softens the form factor significantly ($\delta\alpha_2=1.6$/fm). This tendency is the same for the $^3P_0$-FT model; however, it is opposite in the $^3P_0$-FV model as shown in Table I.

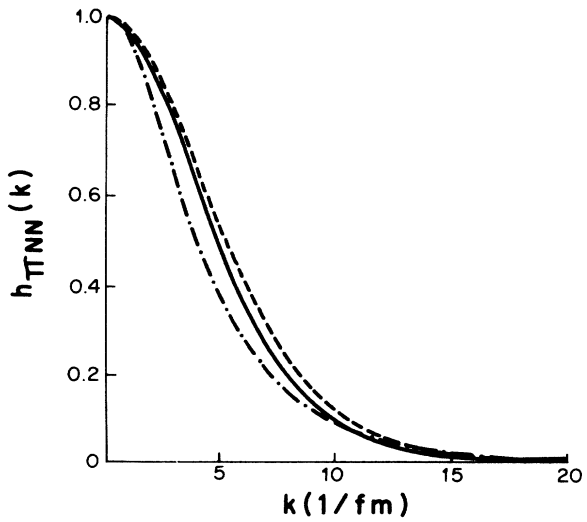

FIG. 6. R_π and $C_{\pi N}$ dependences of the πNN form factor are shown for the $^3S_1$-FT model. The solid line shows the interpolated form factor with $R_\pi=0.29$ fm and $C_{\pi N}=0$ fm ($\alpha_2=7.7$/fm), the dashed line with $R_\pi=0.16$ fm and $C_{\pi N}=0$ fm ($\alpha_2=8.1$/fm), and the dashed-dotted line with $R_\pi=0.29$ fm and $C_{\pi N}=0.288$ fm ($\alpha_2=6.1$/fm).

In this flux-tube model, the Yukawa potential is explained by a piece of the flux-tube breaking off from a nucleon, propagating as a pion, and attaching itself to the other. By deriving a Breit interaction[27] for the process shown in Fig. 7, we obtain the Yukawa potential described by the quark model.

D. Summary

The results discussed above are summarized as follows.

(1) The hard-core size of the final πN interaction, adjusted to explain the πNN coupling constant in the $^3S_1$

model, is consistent with the one (≈ 0.4 fm) used for explaining the S-wave phase shifts. The core size in the $^3P_0$ model is smaller than this.

(2) The $N-\Delta$ mass shift difference depends much on the model; however the results indicate that it could be as large as the $N-\Delta$ mass difference. Therefore, the color coupling constant (α_c), determined by the $N-\Delta$ mass splitting, must be reexamined, and the flux-tube quark-model spectroscopy should be repeated by including these mass shifts.

(3) The cutoff parameter (α_2) of the πNN form factor depends strongly on the final-state interaction rather than on the $q\bar{q}$ creation models.

(4) α_2 in the $^3S_1$ model is consistent with the conventional value (4–6/fm); however, the one in the $^3P_0$ model is larger (≈ 7/fm). $\alpha_2(\pi NN)$ is slightly larger than $\alpha_2(\pi N\Delta)$.

(5) In the analysis of the $\pi N\Delta$ system, it looks like the $^3S_1$-FT-SR model is a suitable model; however, the $^3P_0$-FT-SR model also gives a reasonable description if we choose the pion rms radius as 0.16 fm. The naive $^3P_0$ model obtains the πNN coupling without the final-state interaction as investigated before. In any case, it is still too early to discriminate against these models, and we had better think about other ways to evaluate these models more definitely.

(6) The Yukawa potential is explained by breaking a flux tube from a nucleon and attaching it to another nucleon in the flux-tube quark model.

ACKNOWLEDGMENTS

I am grateful for useful discussions with Professor F. E. Close and Professor V. R. Pandharipande. This research was jointly supported by the National Science Foundation under Contract No. PHY-84-15064, by the Division of Nuclear Physics, U.S. Department of Energy under Contract No. DE-AC05-84OR21400 with Martin Marietta Energy Systems Inc., and by the State of Tennessee Science Alliance Center under Contract No. R01-1061-68.

*Present address: Nuclear Theory Center, 2401 Milo B. Sampson Lane, Bloomington, IN 47408-0768.

[1]A. Chodos *et al.*, Phys. Rev. D **9**, 3471 (1974); **10**, 2599 (1974); T. DeGrand *et al.*, *ibid.* **12**, 2060 (1975); C. DeTar and J. F. Donoghue, Annu. Rev. Nucl. Part. Sci. **33**, 235 (1983).

[2]G. A. Miller *et al.*, Phys. Lett. **91B**, 192 (1980); S. Théberge, A. W. Thomas, and G. A. Miller, Phys. Rev. D **22**, 2838 (1980); A. W. Thomas, S. Théberge, and G. A. Miller, *ibid.* **24**, 216 (1981); S. Théberge *et al.*, Can. J. Phys. **60**, 59 (1982); A. W. Thomas, Adv. Nucl. Phys. **13**, 1 (1983). Reference 25 also investigated pionic effects.

[3]G. E. Brown and M. Rho, Phys. Lett. **82B**, 177 (1979); G. E. Brown, M. Rho, and V. Vento, *ibid.* **84B**, 383 (1979); **97B**, 423 (1980).

[4]J. Carlson, J. B. Kogut, and V. R. Pandharipande, Phys. Rev. D **27**, 233 (1983); **28**, 2807 (1983).

[5]N. Isgur and J. Paton, Phys. Rev. D **31**, 2910 (1985).

[6]J. W. Alcock, M. J. Burfitt, and W. N. Cottingham, Z. Phys. C **25**, 161 (1984); see also E. Eichten, K. Gottfried, T. Kinoshita, K. D. Lane, and T.-M. Yan, Phys. Rev. D **17**, 3090 (1978); **21**, 203 (1980); W. S. Jaronski and D. Robson, *ibid.* **32**, 1198 (1985).

[7]R. Kokoski and N. Isgur, Phys. Rev. D **35**, 907 (1987).

[8]S. Kumano and V. R. Pandharipande, Phys. Rev. D **38**, 146 (1988).

[9]A. Le Yaouanc, L. Oliver, O. Pène, and J.-C. Raynal, Phys. Rev. D **8**, 2223 (1973); **11**, 1272 (1975).

[10]F. Lenz, J. T. Londergan, E. J. Moniz, R. Rosenfelder, M. Stingl, and K. Yazaki, Ann. Phys. (N.Y.) **170**, 65 (1986); S. Kumano and E. J. Moniz, Phys. Rev. C **37**, 2088 (1988).

[11]F. Stancu and P. Stassart, Phys. Rev. D **38**, 233 (1988); **39**, 343 (1989).

[12]G. A. Miller, Phys. Rev. C **39**, 1563 (1989).

[13]F. E. Close, *An Introduction to Quarks and Partons* (Academic, New York, 1979).

[14]D. M. Brink and G. R. Satchler, *Angular Momentum* (Oxford University Press, Cambridge, England, 1968).

[15]V. R. Pandharipande (personal communcations); S. E. Koonin, *Computational Physics* (Benjamin/Cummings, New York, 1986).

[16]J. Hamilton, in *High Energy Physics,* edited by E. H. S. Burhop (Academic, New York, 1967).

[17]S. Kumano, Phys. Lett. B **214**, 132 (1988); Nucl. Phys. **A495**, 611 (1989).

[18]N. A. Törnqvist, Phys. Lett. B **221**, 701 (1989).

[19]L. Heller, S. Kumano, J. C. Martinez, and E. J. Moniz, Phys. Rev. C **35**, 718 (1987).

[20]For numerical evaluations, see K. T. R. Davies, J. Phys. G **14**, 973 (1988); G. D. White, K. T. R. Davies, and P. J. Siemens, Ann. Phys. (N.Y.) **187**, 198 (1988).

[21]N. Isgur and G. Karl, Phys. Rev. D **19**, 2653 (1979); **20**, 1191 (1979); S. Godfrey and N. Isgur, *ibid.* **32**, 189 (1985).

[22]D. P. Stanley and D. Robson, Phys. Rev. D **21**, 3180 (1980).

[23]J. A. Johnstone and T.-S. Lee, Phys. Rev. C **34**, 243 (1986).

[24]R. L. Jaffe and F. E. Low, Phys. Rev. D **19**, 2105 (1979); A. K. A. Macial and J. E. Paton, Nucl. Phys. **B181**, 277 (1981).

[25]Y. Nogami and N. Ohtsuka, Phys. Rev. D **26**, 261 (1982).

[26]K. Holinde, Phys. Rep. **68**, 121 (1981).

[27]J. J. Sakurai, *Advanced Quantum Mechanics* (Benjamin/Cummings, New York, 1967).